HiSST: International Conference on High-Speed Vehicle Science Technology
26–29 November 2018, Moscow, Russia

Combined approach on the aerodynamic shape optimization

Nikita D. Ageev[1], Alexander A. Pavlenko[2]

Abstract

At the present time two main approaches to aerodynamic shape optimization may be distinguished. The first approach requires only direct calculations. The second one expects the availability of tools for the evaluation of the constraint and objective function gradients. The first approach is robust and has opportunities for the topological optimization. The second one allows to operate with large number of design variables. To achieve high aerodynamic efficiency, it is proposed to combine these approaches in two-stage optimization process. The purpose of the work is the development of this technique. The planar inviscid symmetric problem of the optimization of the constrained area airfoil with sharp leading edge is solved. The results are in good agreement with the data previously obtained by other researchers. The relative drag residual equals 1%. The developed technique is used for aerodynamic optimization of the body of revolution at Mach number of 1.8. The Sears-Haack body is used as a baseline configuration. The body shape variation is realized at the first stage with the deforming spline through 5 points and at the second stage with the free-form deformation box of 101x2 control points. Flow simulation is carried out by way of the numerical solution of RANS equations with closure of differential turbulence models SA and SST. The continuous adjoint solver is used for gradient evaluation. Heuristic algorithm of indirect optimization based on self-organization is involved at the first stage and sequential quadratic programming – at the second stage. Total drag reduction of 22% is reached (19% at the first stage, 3% at the second stage). Drag reduction is achieved due to the volume transfer from front part of the body to the rear one at both stages.

Keywords: *aerodynamic shape optimization, adjoint solver, RANS, body of revolution*

Nomenclature

M – Mach number
Re – Reynolds number over the body length
P – static pressure
P∞ - far field static pressure
L – body length
X – longitudinal coordinate over the body length
R – local body of revolution radius
CD – drag coefficient

1. Introduction

It is required to reach high fuel efficiency and range in the supersonic aircraft design. Aerodynamic efficiency is the key component for the solution of these problems. Thus, aerodynamic shape optimization techniques that are part of the aerodynamics design techniques set (Fig. 1) are subjects of special interest. There are two major aerodynamic shape optimization approaches. In the first approach only direct flow simulation is required (tagged by yellow rectangle in figure 1). The second one is based on the use of tools that allow to evaluate the gradients of the cost function in single simulation (marked with a red rectangle).

[1] *TsAGI, MIPT, Moscow, n.d.ageev@gmail.com*
[2] *TsAGI, MIPT, Moscow, alexander.a.pavlenko@gmail.com*

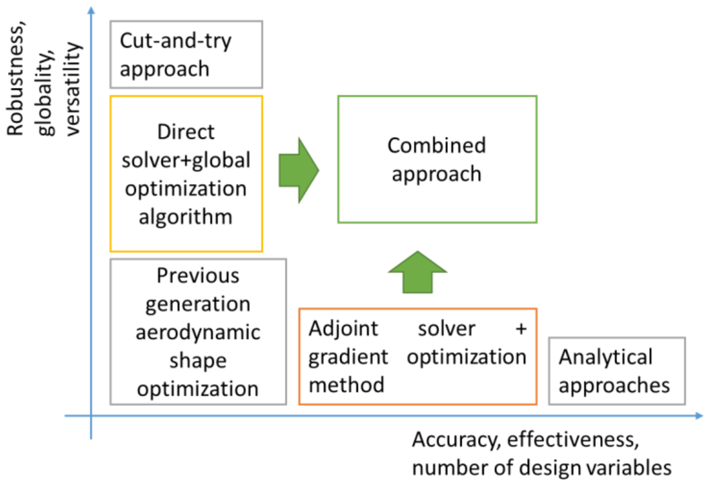

Fig 1. Aerodynamic design techniques

Methods of the first type suffer from the so-called "curse of dimensionality". When the number of parameters grows linearly, the volume of the optimization space grows exponentially. This results in an increase in the number of direct solver calls. With a single optimum in the optimization area, the number of calls is O (n ^ 2). In the most general case, O (2 ^ n), that results in a dramatic increase of the optimization time. To partially solve this problem, one can use high-performance heuristic optimization algorithms (such as [1, 2]) and fast evaluation methods [3, 4, 5]. Fast evaluation methods are usually based on low-fidelity models or use approximations of high-fidelity simulation results. Heuristic algorithms require testing. On the other hand, the first approach techniques are robust and suitable for topological optimization [6]. It is possible to optimize functionals that have discontinuities and non simply connected domains of definition. When the mesh techniques are used, methods of the first type make it possible to soften the requirements for the computational mesh. In addition, it is possible to implement algorithms for constructing a computational grid, which minimize the influence of the computational grid on the results. Solvers on Cartesian computational grids are promising for use in methods of the first type [7]. The genetic algorithm [8] is universal and can be used as an optimizer. Techniques of the first approach allow to find a global maximum.

Techniques of the second type, on the contrary, make it possible to overcome the "curse of dimensionality" and achieve fast convergence. To use them, one must have tools for rapid calculation of the functional variations. Adjoint solver [9] or local linearization [10] can be applied. However, they have difficulties with the search of global extremum, operation with discontinuous functions, functions with non-simply connected domains of definition. When using mesh methods, usually computational grid deformation technologies are used coupled with tools for the functional variation evaluation. The effect of grid distortion may exceed the effect of changes in boundary conditions at significant mesh deformation. This may result in incorrect results. The use of continuous adjoint solver technologies also imposes increased requirements on the quality of the computational grid.

Thus, it is rational to combine the techniques of the described classes. In this case, you should first perform a global search with first approach techniques, and then local - with second approach techniques. An iterative process can be organized. This paper describes the experience of applying the combined approach to the problem of optimizing the shape of two-dimensional configurations at supersonic speeds.

2. Problem formulations and methodology

2.1. Problem formulations

The problem of the symmetric airfoil optimization in viscous supersonic flow is the test case (problem (a)). Mach number equals 3. Airfoil chord length is equal to 1. Airfoil area is constrained and equals 0.19246. Leading edge is sharp. Trailing edge base pressure is fixed as $P=P_{\infty}$. The solution of this problem is described by Takovitskii [11] and Kraiko [12].

The body of revolution optimization problem in the supersonic viscous flow (problem (b)) is formulated for further technique development. The volume of body equals 1% from cubed length. Mach number is 1.8, Re number is 165 millions. Leading and trailing base areas aren't constrained.

2.2. Methodology

The general scheme of the solution is presented in Figure 2. At stage 1, optimization is carried out using an exclusively direct flow simulation. The highly efficient IOSO optimization algorithm described in [1], based on the parameter variation limits and search history, forms a set of input parameters. This set is fed to the input of a calculation procedure built using the toolkit of the commercial software package ANSYS. The procedure includes the generation of geometry, mesh and subsequent numerical simulation of the flow. The drag coefficient is determined using numerical simulation and returned to the optimizer. The area (volume) of the airfoil (body) is calculated analytically using the trapezoidal method (truncated cones method). The optimization algorithm automatically decides on the need for additional calculations in the vicinity of the current optimum, and also predicts the position of the new optimum based on the approximation. The process continues until convergence. The optimal airfoil (body) obtained at the first stage acts as a base configuration for stage 2. The second optimization stage is carried out in the software package with open source code SU2 [13]. At the second stage, the optimization problem formulation is performed and then control script written in the Python programming language shape_optimization.py is run. This script starts the direct solver, the adjoint solver, the system for calculating geometric parameters, the gradient recalculation system, and transfers the obtained parameters to the optimizer based on the gradient sequential quadratic programming method (SLSQP) from the open-source library SciPy [14]. SU2 does not provide the calculation of the open loop area and the volume of the axisymmetric configuration; therefore, two modifications and reassembly of the code in the C ++ programming language are performed. The build is carried out using the Cmake 3.8.2 build automation system by the MinGW-64 4.3.0 compiler. When solving the problem (a), the Compute_Area function (geometry_structure.cpp file) returned the area under the planar curve, and when solving the problem (b), the volume of the axisymmetric body.

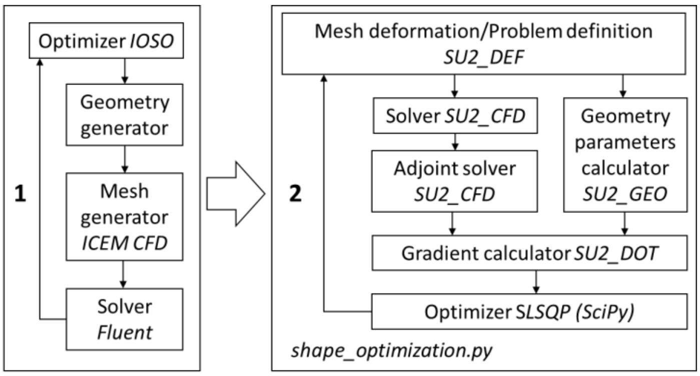

Fig 2. Workflow

The problems used model of compressible ideal gas. In problem (a) the gas is non-viscous, the Euler equations are solved. In problem (b) the gas is viscous, the RANS equations are solved. The closure is made with the SST turbulence model at the first stage and Spallart-Allmaras model at the second one. The degree of influence of the turbulence model on the optimization results is evaluated in comparison with the optimization problem solution in the framework of the Euler equations of 1% of the drag coefficient.

At the first stage of optimization, the number of parameters should be reasonably limited. Therefore, a parameterization scheme using a deforming spline is selected. The spline coordinate is added to the vertical coordinates of the base configuration. The fifth order spline was used, passing through 5 control points. Control points are uniformly distributed along the length of the body. The parabolic profile was chosen as the base configuration for problem (a), and the Sears – Haack body was chosen for problem (b).

At stage 2, the parameterization using the free-form deformation box is applied. A box is created around the deformable object, and control points are placed on the box surface and inside of it with a certain step. These points are free to move. In this work, the points are placed on the edges of the box, the step is uniform, and control points can only move along the vertical axis. On the vertical faces of the point are located exclusively in the corners of the box, the step of placing the points horizontally - 0.04 for the task (a) and 0.01 - for the task (b). The space between the points is deformed according to the principle of a linearly elastic material.

Thus, the number of variable parameters is five for the first stage of optimization in both tasks, 25 (including the pointed nose) for the second stage of task b, 101 for the second stage of task a.

The calculation grids used in the work are structured multiblock meshes. The grids are shown in Figure 2 and systematized according to the tasks and stages at which they are applied. The computational grid a-1 is uniform, with H-topology, has 100 cells along the chord of the profile. The total number of nodes is 22952. The computational grid a-2 has the O-topology, 31,200 nodes. The computational grid for problem b did not change when going from stage 1 to stage 2, and has 54080 computational nodes. Calculation grids are prepared in ANSYS ICEM CFD. The restructuring of the grid during the first stage of optimization is performed by executing a script for ICEM CFD, written in the Tk/Tcl programming language.

For the first stage of optimization, the Ansys Fluent solver is used in both problems, for the second one - SU2. The design scheme is implicit in all solvers.

At stage 1 of problem (a), the Euler equations are solved. We used a density-based solver with Roe flow calculation, a first-order upwind scheme. The Courant number is 0.5, convergence is achieved in 10 thousand iterations. At stage 1 of problem (b), the Reynolds equations are numerically solved with the closure by the Menter turbulence model k-ω SST with a completely turbulent boundary layer. The method of solution Reynolds equations is pressure-based, coupled with approximation of the second order of all equations. During the solution, the average Courant number is 5. The problem is solved in 1400 iterations. The first 200 iterations of the temperature relaxation parameter, which limits rapid temperature changes in the solution, is equal to 0.5, the next 1200 - 1.

The settings of the direct solver SU2 in problem (a) are the following: the convective flows are determined using the Roe method, the 2nd order scheme. Implicit Euler scheme in time, Courant number 1. A geometric multigrid method of level 2, working by the V-cycle. The continuous adjoint solver also used the Roe method, started with a Courant number of 0.8 without using the multigrid method and used a 1st order scheme. The convergence criterion is a decrease in the residuals by 10 orders compared with the 10th iteration. In problem (b), the closure of the Reynolds equations is carried out using the S-A model. Courant number was 3 units. The flow approximation is performed according to the JST scheme, for spatial integration a second-order scheme is used with the Bart-Jespersen limiter for the equations of momentum, mass and energy and the first order for the equations of the turbulence model. The implicit Euler scheme is applied for the time approximation. The direct method in problem (b) does not use the multigrid approach. The continuous adjoint solver in problem (b) used the first order scheme and the multigrid method of level 3, working on the W-cycle. The convergence in problem (b) is controlled by the Cauchy criterion (the deviation is smaller than 0.0005 per 1000 iterations).

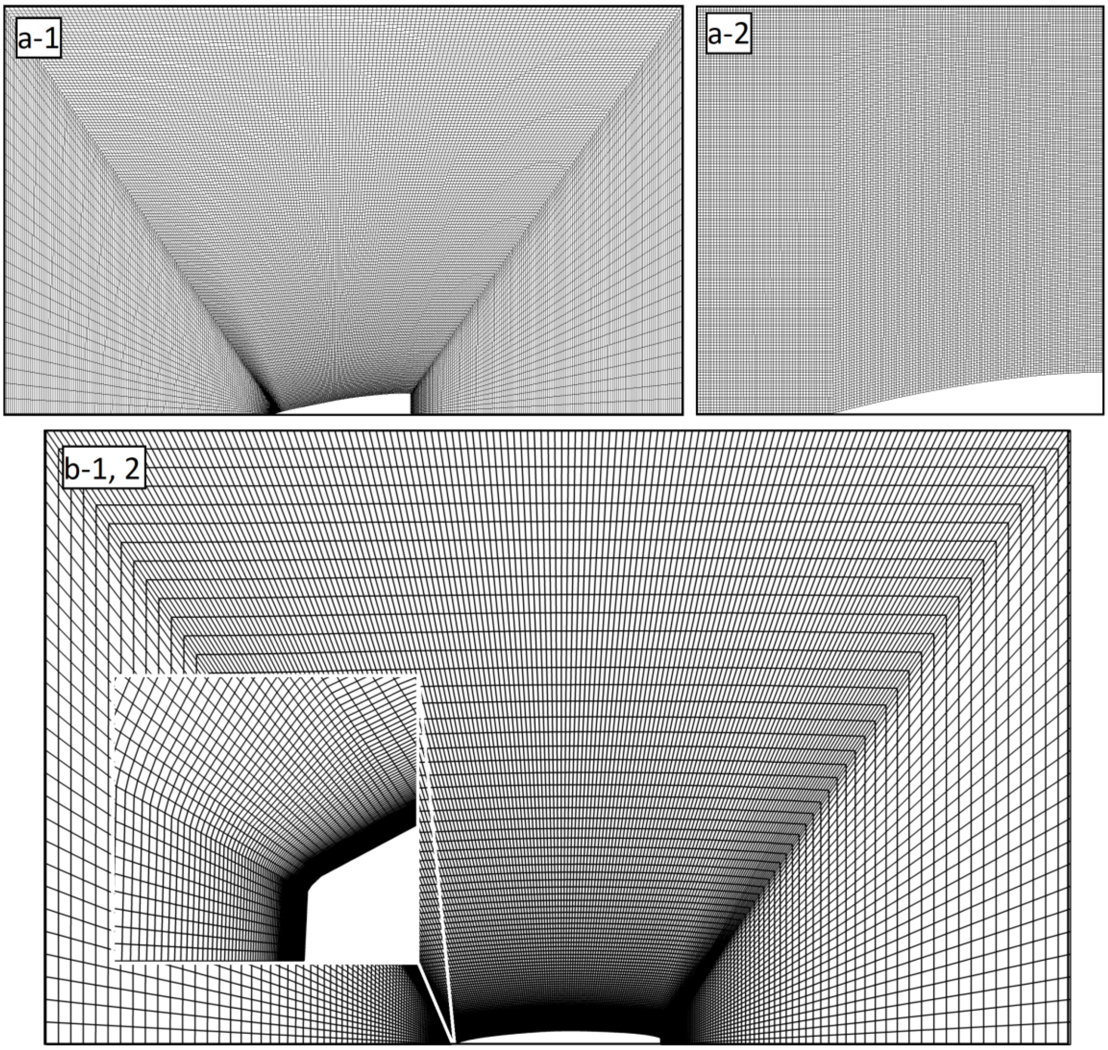

Fig 3. Meshes

The calculation of the area in problem (a) and volume in problem (b) iss performed numerically using the first order method using the coordinates of the computational grid nodes belonging to the surface of the body under study.

3. Results and discussion

The first stage of optimization required a global iteration for problem (a) 121 (Figure 4). A significant decrease in drag is noticeable; it causes by the possibility of independent variation of parameters in wide ranges. The second stage of solving problem (a) required 24 global iterations and led to a decrease in the drag coefficient compared to the result of the first stage by about 1 percent (Figure 5).

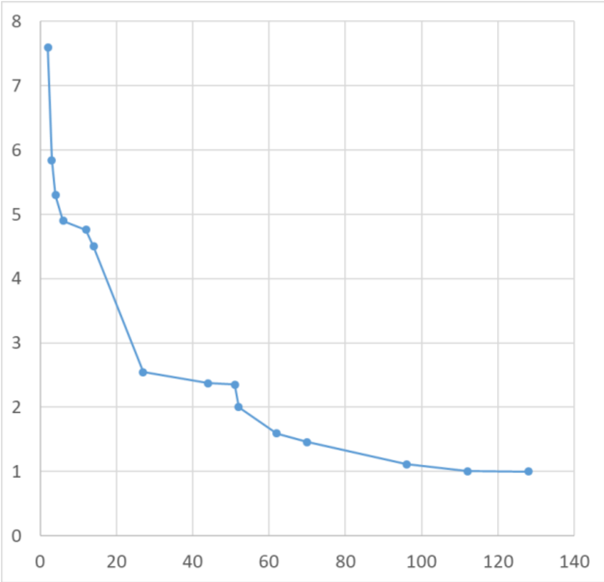

Fig 4. The relative drag as function of the iteration number at the first stage of solving problem (a)

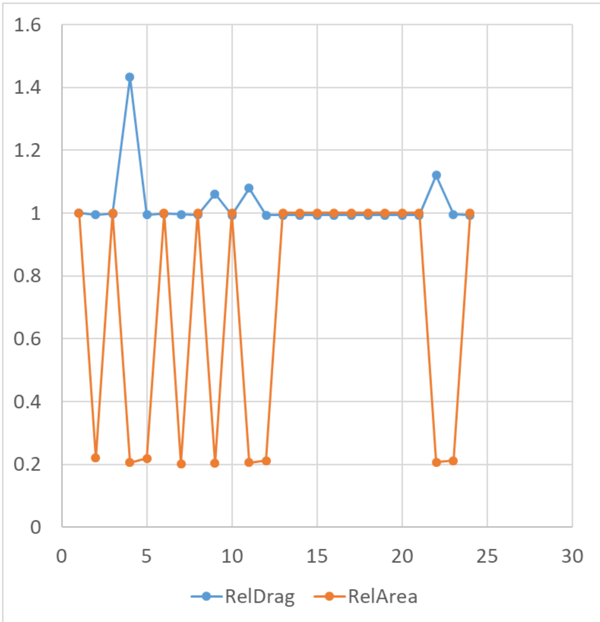

Fig 5. The relative drag and airfoil area as function of the iteration number in the second stage of solving the problem (a)

The shape of the airfoil in comparison with the well-known result S.A. Takovitskii shown in Figure 6. Established a good agreement of the results obtained as a result of data optimization. Relative difference between the corresponding results is 1%.
The graph of convergence has a number of sharp bursts that, apparently, demonstrates the need for a more precise adjustment of the optimization algorithm. Nevertheless, second stage of optimization improves the correspondence of local slopes to a known result (Figure 7).

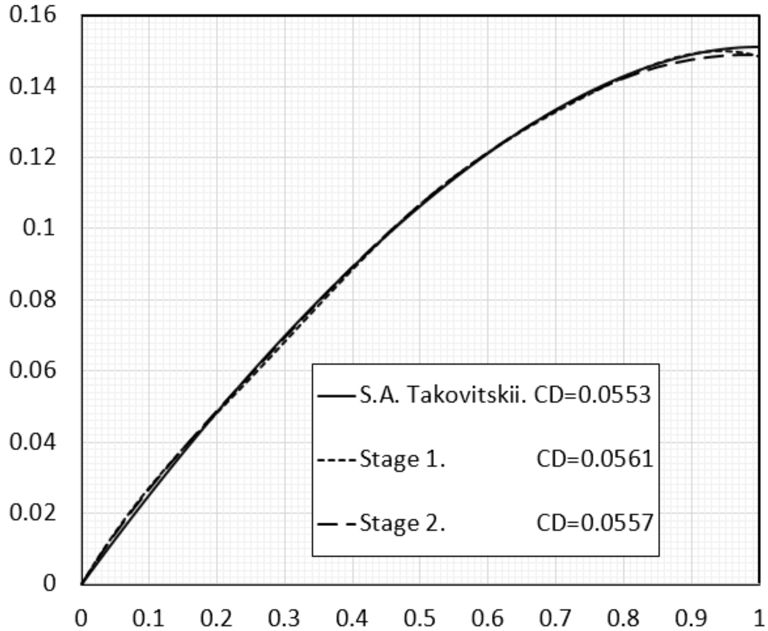

Fig 6. Optimal airfoil shapes, obtained by solving the problem (a).

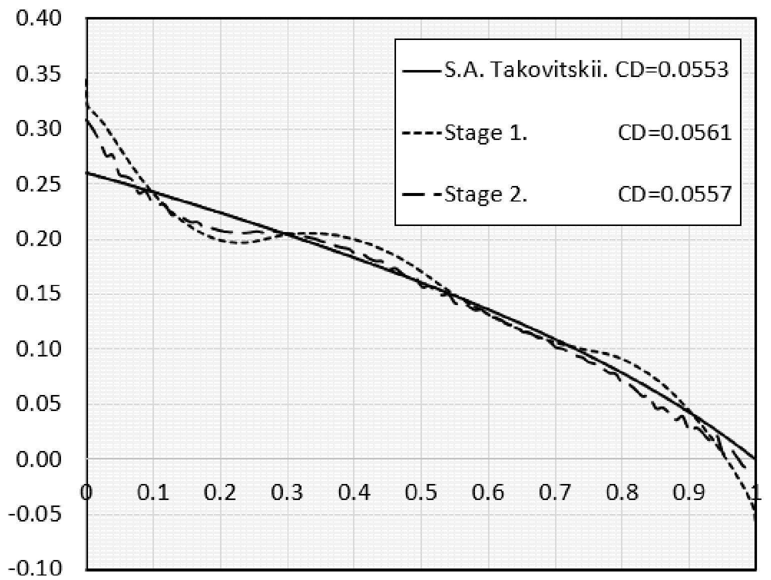

Fig 7. The slopes of the optimal airfoil surfaces as function of the X coordinate - problem (a).

Moreover, the distribution of Mach numbers and pressure ratio (Figure 8) also show a decrease in spatial oscillations of flow parameters around the airfoil.

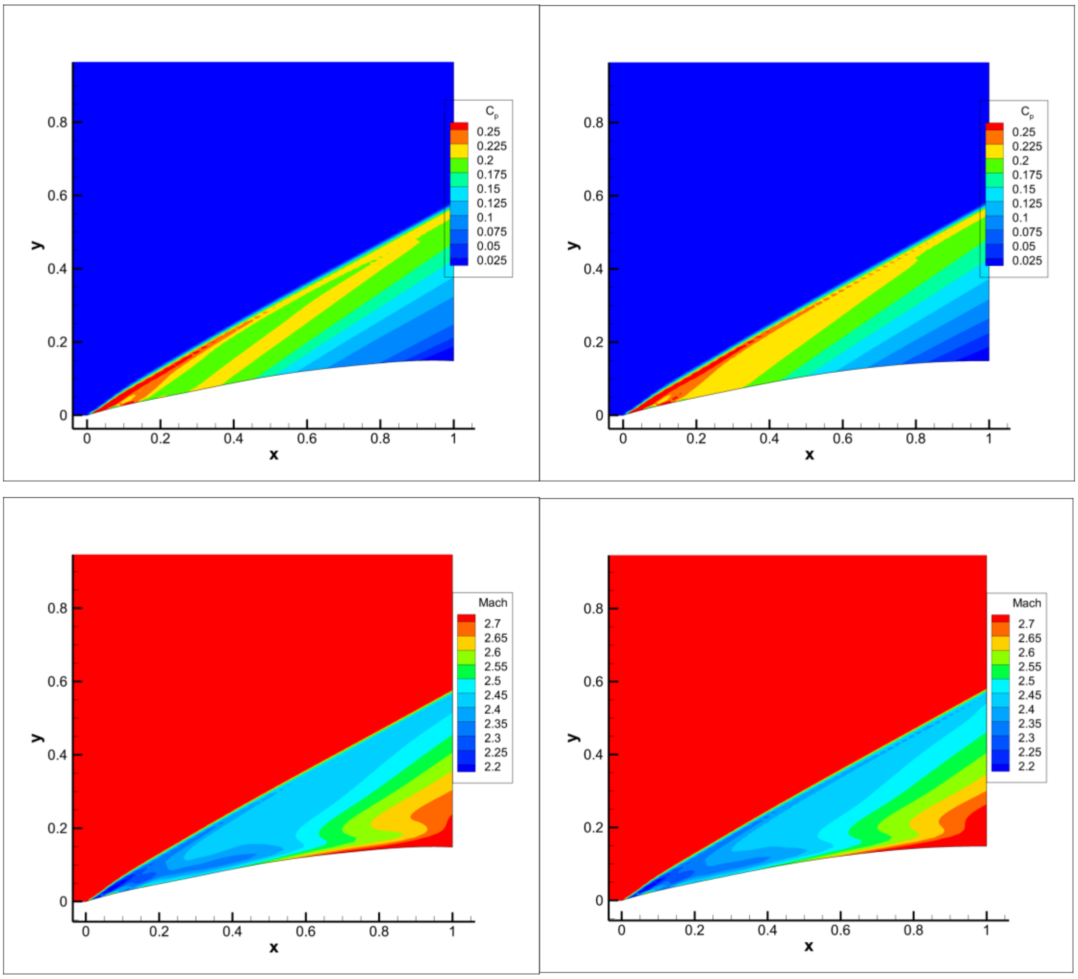

Fig 8. The pressure coefficient and Mach number fields around airfoil obtained as a result of the first (left) and second (right) optimization stage in problem (a)

The first stage of optimization requires 64 global iterations for problem (b) (Figure 9). At the second stage, 61 global iterations are required (Figure 10). The shapes of the optimal bodies are shown in Figure 11. At the same time, the drag of the body of revolution is reduced in comparison with the body of Sears-Haack totally by 22%, 19 of them are obtained at the first stage. During the first stage of solution a viscous axisymmetric optimization problem, we managed to reduce the drag coefficient of the body of revolution by 19%. Such a significant decrease is associated with the formation of the bases and the transfer of body volume from the nose part of the body to the rear base. This fact is demonstrated by the distribution of velocities and pressure coefficients shown in Figures 12, 13. The qualitative features of the solution to the optimization problem in the framework of the Euler equations are also preserved in the axisymmetric case. During the second stage of the solution, the variation in the shape of the body is the same as in the first. A further decrease in drag in the second stage is apparently concerned with to the presence of the "bad legacy" of the Sears-Haack body in the first stage result. Namely, the Sears-Haak body has an infinite negative angle of inclination in the region of its rear end. This leads to the formation of local separations in the aft part of the body. You can reduce the size of the separation zone and at the same time add volume to the rear part of the body. This will reduce the local angles of inclination in front of the body while maintaining volume. Integrally, this leads to a decrease in resistance by an additional 3%.

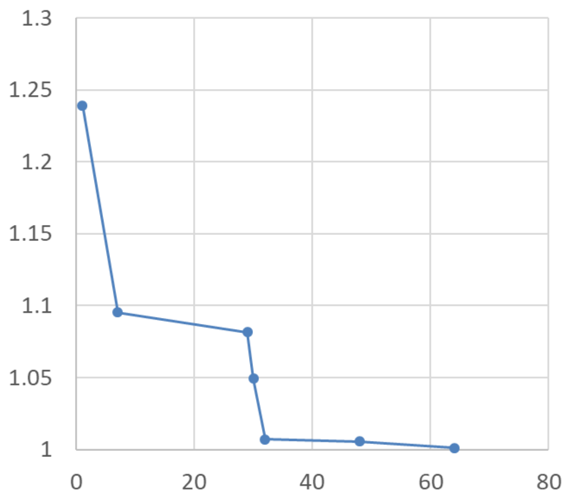

Fig 9. The relative drag as function of the iteration number at the first stage of problem (b) solution

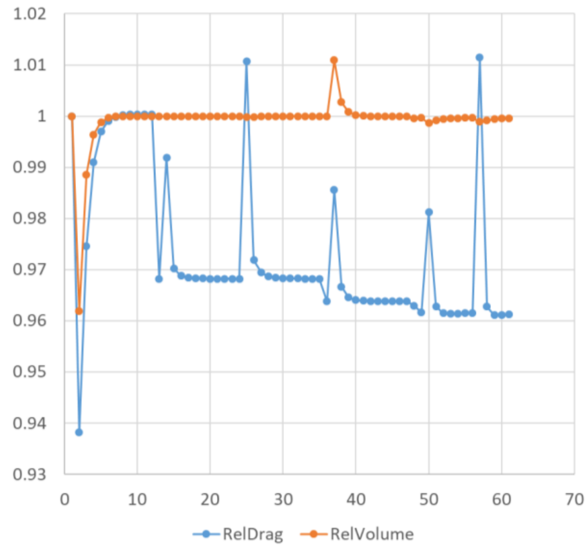

Fig 10. The relative drag and volume as function of the iteration number at the second stage of the problem (b) solution

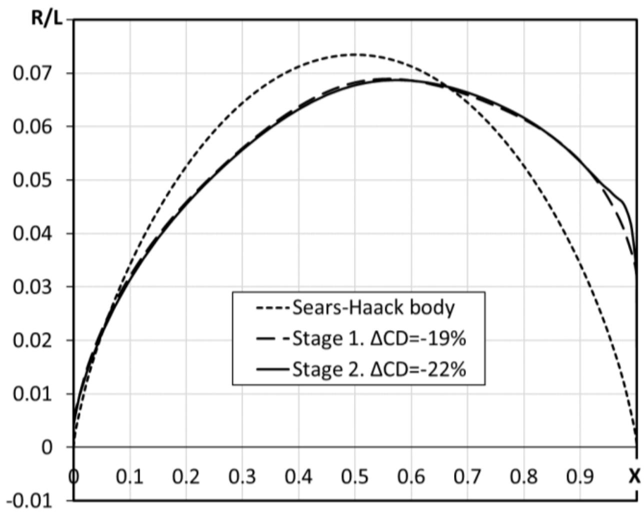

Fig 11. Optimal body shapes in problem (b) solution

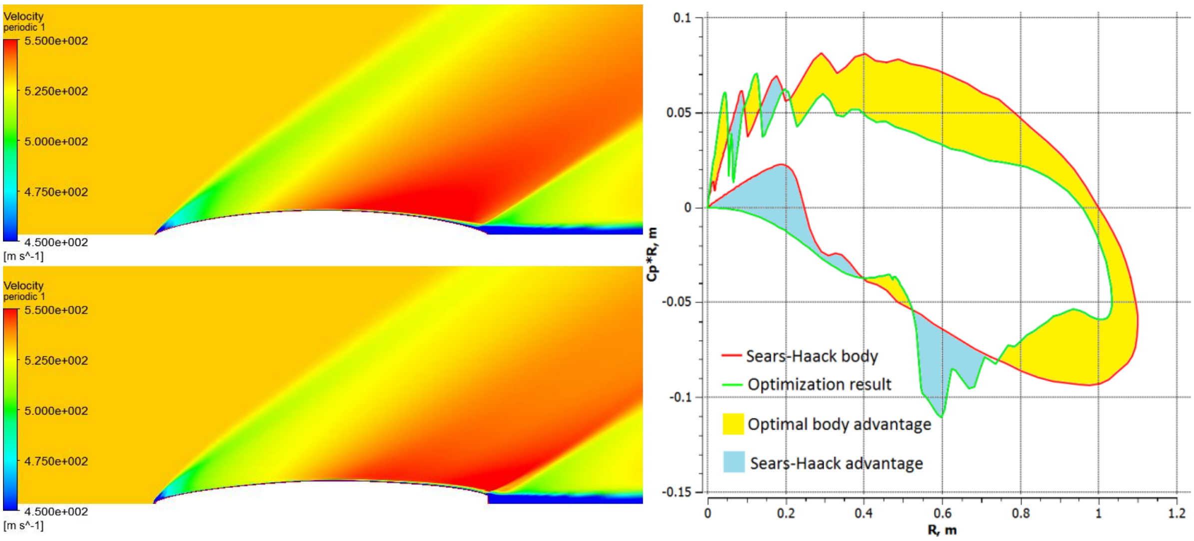

Fig 12. Velocity and the pressure coefficient multiplied by the radius around the Sears-Haack body and the result of the first optimization stage.

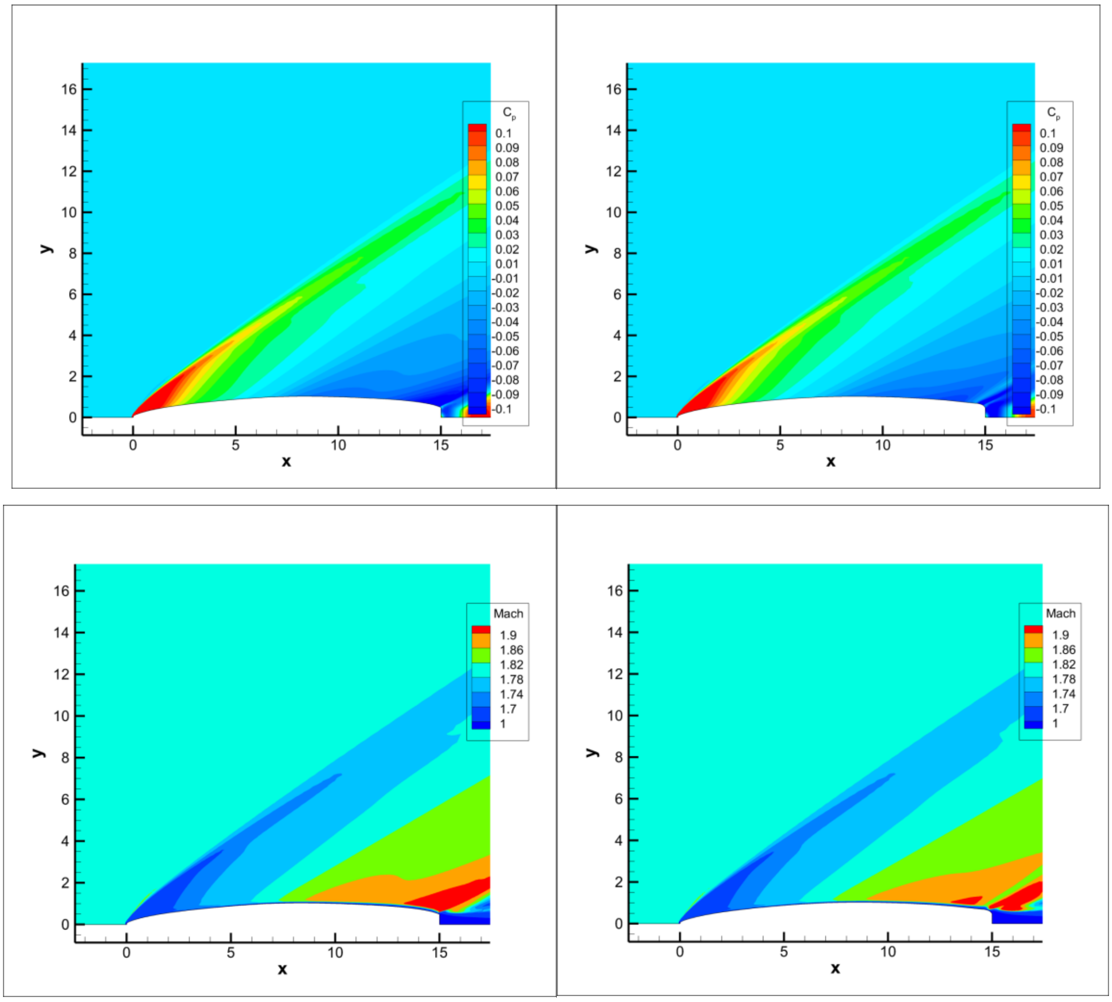

Fig 13. The pressure coefficient and Mach number fields around airfoil obtained as a result of the first (left) and second (right) optimization stage in problem (b)

4. Conclusion

A new approach that allows increasing the versatility, robustness and accuracy of the optimization procedure is proposed. These features are necessary for solution of complex problems of aerodynamic design. In this paper, two test problems of aerodynamic optimization are solved. The application of the new approach has shown adequate results. In combination with a discretely coupled solver and efficient global optimization algorithms, this approach will effectively solve a new class of problems, including aerodynamic topological optimization problems and optimization problems for complex aircraft designs.

References

1. Egorov, I., Kretinin, G., Leshchenko, I., & Kuptzov, S. (2002, September). IOSO optimization toolkit-novel software to create better design. In 9th AIAA/ISSMO Symposium on Multidisciplinary Analysis and Optimization (p. 5514).
2. Lotov, A.V. & Pospelov, A.I. Dokl. Math. (2007) 75: 460. https://doi.org/10.1134/S1064562407030349
3. Bernstein, A. V., Kuleshov, A., Sviridenko, Y., & Vyshinsky, V. (2007, November). Fast aerodynamic model for design technology. In Proceedings of West-East High Speed Flow Field Conference (WEHSFF-2007), Moscow, Russia.
4. Drela, M. (1989). XFOIL: An analysis and design system for low Reynolds number airfoils. In Low Reynolds number aerodynamics (pp. 1-12). Springer, Berlin, Heidelberg.
5. Karas, O., & Kovalev, V. (2012). Fast CFD Algorithms for Steady and Unsteady Problems of Practical Aerodynamics. In 11th ONERA-TsAGI Seminar on" Advanced research in aerodynamics (pp. 9-12).
6. Othmer, C., Manosalvas-Kjono, D. E., Jameson, A., & Alonso, J. J. (2017). Aerodynamic Topology Optimization: Some Observations on Hysteresis. In 23rd AIAA Computational Fluid Dynamics Conference (p. 4413).
7. Aksenov, A. A., Kharchenko, S. A., Konshin, V. N., & Pokhilko, V. I. (2004). -FlowVision software: Numerical simulation of industrial CFD applications on parallel computer systems. In Parallel Computational Fluid Dynamics 2003 (pp. 401-408).
8. Quagliarella, D., & Della Cioppa, A. (1995). Genetic algorithms applied to the aerodynamic design of transonic airfoils. Journal of aircraft, 32(4), 889-891.
9. Jameson, A., Martinelli, L., & Pierce, N. A. (1998). Optimum aerodynamic design using the Navier–Stokes equations. Theoretical and computational fluid dynamics, 10(1-4), 213-237.
10. Takovitskii, S. A. (2006). Analytical solution in the problem of constructing axisymmetric noses with minimum wave drag. Fluid Dynamics, 41(2), 308-312.
11. Takovitskii, S. A. (2003). Analytic solution in the problem of constructing an airfoil with minimum wave drag. Fluid dynamics, 38(6), 933-941.
12. Kraiko, A. N., & Pudovikov, D. Y. (1997). The role of a length constraint in the design of minimum-drag bodies. Journal of applied mathematics and mechanics, 61(5), 797-810.
13. Economon, T. D., Palacios, F., Copeland, S. R., Lukaczyk, T. W., & Alonso, J. J. (2015). SU2: an open-source suite for multiphysics simulation and design. AIAA Journal, 54(3), 828-846.
14. Jones, E., Oliphant, T., & Peterson, P. (2014). {SciPy}: open source scientific tools for {Python}.